

Different binding modes of tropeines mediating inhibition and potentiation of $\alpha 1$ glycine receptors

Gábor Maksay,*†‡ Rudolf Schemm,§ Joanna Grudzinska,†¹ Malgorzata Drwal† and Heinrich Betz†

*Department of Molecular Pharmacology, Institute of Biomolecular Chemistry, Chemical Research Center, Hungarian Academy of Sciences, Budapest, Hungary

†Department of Neurochemistry, Max-Planck-Institute for Brain Research, Frankfurt/Main, Germany

‡AG Zelluläre und molekulare Neurophysiologie, Technische Universität Darmstadt, Darmstadt, Germany

§Department of Theoretical and Computational Biophysics, Max-Planck-Institute for Biophysical Chemistry, Göttingen, Germany

Abstract

Tropeines are bidirectional modulators of native and recombinant glycine receptors (GlyRs) and promising leads for the development of novel modulatory agents. Tropisetron potentiates and inhibits agonist-triggered GlyR currents at femto- to nanomolar and micromolar concentrations respectively. Here, the potentiating and inhibitory effects of another tropeine, 3 α -(3'-methoxy-benzoyloxy)nortropine (MBN) were examined by voltage-clamp electrophysiology at wild type and mutant $\alpha 1$ GlyRs expressed in *Xenopus laevis* oocytes. Several substitutions around the agonist-binding cavity of the $\alpha 1$ subunit interface (N46C, F63A, N102A, R119K, R131A, E157C, K200A, Y202L and F207A) were found to reduce or eliminate MBN inhibition of glycine activation. In contrast, the binding site mutations Q67A, R119A and S129A which did not affect MBN inhibition abolished the potentiation of chloride

currents elicited by low concentrations of the partial agonist taurine following pre-incubation with MBN. Thus, potentiation and inhibition involve distinct binding modes of MBN in the inter-subunit agonist-binding pocket of $\alpha 1$ GlyRs. Homology modelling and molecular dynamics simulations disclosed two distinct docking modes for MBN, which are consistent with the differential effects of individual binding site substitutions on MBN inhibition and potentiation respectively. Together these results suggest that distinct binding modes at adjacent binding sites located within the agonist-binding pocket of the GlyR mediate the bidirectional modulatory effects of tropeines.

Keywords: inhibition, ligand docking, molecular dynamics simulation, potentiation, tropeine binding, $\alpha 1$ glycine receptors.

J. Neurochem. (2009) **109**, 1725–1732.

Glycine is the major inhibitory neurotransmitter in spinal cord and brain stem (Aprison 1990). There, glycinergic synapses control motor and sensory pathways by activating strychnine-sensitive glycine receptors (GlyRs) which belong to the 'Cys-loop' family of ligand-gated ion channels (Laube *et al.* 2002; Lynch 2004). Five GlyR subunit genes ($\alpha 1$ –4 and β) have been identified by molecular cloning. Upon heterologous expression, α subunits, but not β , form functional homopentameric chloride channels. In adult spinal cord, GlyRs are mainly heteropentamers composed of two $\alpha 1$ and three β subunits (Grudzinska *et al.* 2005), whereas at birth homomeric $\alpha 2$ GlyRs prevail (Becker *et al.* 1988). GlyRs containing $\alpha 3$ subunits participate in central inflammatory pain sensitization (Harvey *et al.* 2004).

Agonist-induced GlyR currents can be modulated by different allosteric agents or 'modulators' (reviewed in

Laube *et al.* 2002). However, most of these modulators, such as anaesthetic alcohols, neurosteroids, Zn²⁺ and tropeines, are not GlyR-selective but similarly affect the responses to A-type GABA (GABA_A) receptors (Laube *et al.* 2002) or

Received March 6, 2009; accepted March 26, 2009.

Address correspondence and reprint requests to Dr Gábor Maksay, Chemical Research Center, Hungarian Academy of Sciences, PO Box 17, H-1525 Budapest, Hungary. E-mail: maksay@chemres.hu

¹The present address of Joanna Grudzinska is the School of Biomolecular and Biomedical Research, Conway Institute, University College Dublin, Belfield, Dublin 4, Ireland.

Abbreviations used: 5-HT₃ receptor, type-3 5-hydroxytryptamine receptor; AChBP, acetylcholine binding protein; GABA_A, A-type GABA; GlyR, glycine receptor; LBD, ligand-binding domain; MBN, 3 α -(3'-methoxy-benzoyloxy)nortropine; MD, molecular dynamics; Rg, radius of gyration; wt, wild type.

act at type-3 5-hydroxytryptamine (5-HT₃) receptors (Chesnoy-Marchais 1996). Notably, several GlyR modulatory compounds such as tropeines, dihydropyridines and cannabinoids (Yang *et al.* 2008) produce bidirectional effects: high-affinity potentiation and low-affinity inhibition. For Zn²⁺, both potentiation and inhibition of GlyRs involve binding to the extracellular ligand-binding domain (LBD) which, like those of the other Cys-loop receptors, is homologous to molluscan acetylcholine binding proteins (AChBPs) (Brejc *et al.* 2001; Celie *et al.* 2004). Site-directed mutagenesis and homology modelling based on the structure of AChBP have allowed assigning residues of the $\alpha 1$ GlyR implicated in glycine and strychnine binding to the agonist-binding pocket located between subunit interfaces (Grudzinska *et al.* 2005). This binding pocket is positionally conserved in the Cys-loop receptor family and formed by distinct extracellular segments of the LBD [loops A, B and C on the (+), and loops D, E and F on the (-), sides of the binding interface; see Changeux and Taly 2008]. Notably, the GlyR residues mediating Zn²⁺ potentiation and inhibition also are located within this agonist-binding site (Nevin *et al.* 2003; Grudzinska *et al.* 2008). In contrast, inhaled anaesthetics are thought to bind in a cavity located between the transmembrane domains of the receptor (Beckstead *et al.* 2002).

Amongst the GlyR modulators investigated so far, tropeines have gained particular attention. Originally identified as 5HT₃ receptor antagonists, these compounds were found to potentiate GlyR currents at low, non-saturating agonist concentrations (Chesnoy-Marchais 1996). Subsequently, amides and esters of 3 α -hydroxy-tropane have been shown to display very high affinity to GlyRs (Maksay *et al.* 1998, 2004). Nortropeines like 3 α -(3'-methoxy-benzoyloxy)nortropane (MBN, Fig. 1a), nor-O-zatosestron and nortropisetron displace [³H]strychnine binding to native rat striatal (Maksay *et al.* 2004) and recombinant human $\alpha 1$ (Maksay *et al.* 2008) GlyRs at nanomolar concentrations. Moreover, tropisetron (Fig. 1a) has been shown to potentiate $\alpha 1$ GlyR currents in the femtomolar concentration range (Yang *et al.* 2007). Thus, some tropeines are excellent in displaying both bidirectional modulatory properties and high-affinity binding.

Different lines of evidence indicate that tropeines bind close to or within the agonist/antagonist binding sites of GlyRs. First, Yang *et al.* (2007) identified residue N102 located close to the subunit interfaces as a major determinant of tropisetron inhibition of the $\alpha 1$ GlyR. Second, binding of the structurally related 5HT₃ receptor antagonist granisetron is thought to occur within the agonist-binding cleft of the 5HT₃ receptor (Joshi *et al.* 2006), and the pharmacophores proposed for 'setron-type' 5-HT₃ receptor antagonists and GlyR modulatory tropeines display considerable resemblance (Maksay *et al.* 2004). Here, we examined the effects of binding site mutations in the $\alpha 1$ GlyR on inhibition and potentiation by MBN. Our data are consistent with adjacent

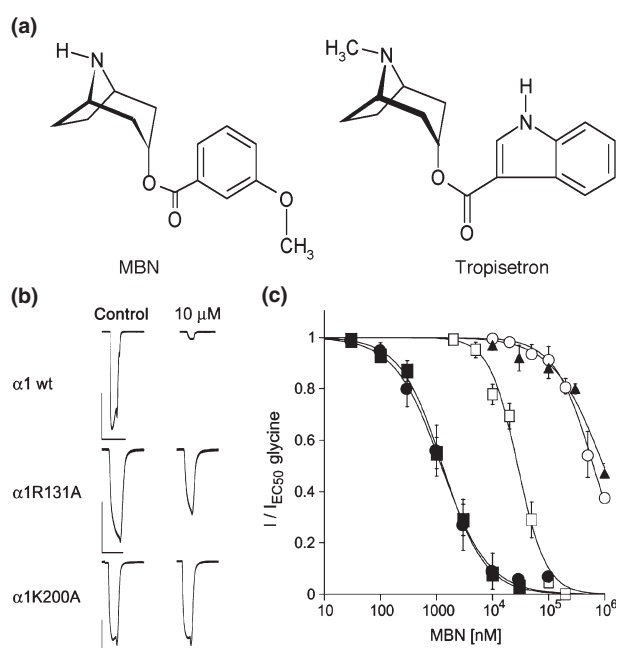


Fig. 1 3 α -(3'-methoxy-benzoyloxy)nortropane (MBN) inhibition of wt and mutant $\alpha 1$ GlyRs. (a) Chemical structures of MBN and tropisetron. (b) Representative current traces reveal a reduced inhibition of the R131A and K200A GlyRs by 10 μ M MBN. The scale bars correspond to 30 s and 2 μ A. (c) Concentration dependence of MBN inhibition for wild type (wt) (■), F63A (▲), R65A (●), R131A (□) and K200A (○) GlyRs. Data are mean \pm SEM from 5 to 10 oocytes.

binding sites and distinct binding modes mediating tropeine potentiation and inhibition.

Materials and methods

Materials

Taurine, collagenase and urethane were obtained from Sigma Chemical Co. (St Louis, MO, USA). MBN was synthesized by Professor Péter Nemes (Szent István University, Budapest) as described (Maksay *et al.* 2004). The point mutations of the human $\alpha 1$ subunit have been described previously (Grudzinska *et al.* 2005). Linearized plasmid DNAs of the wild type (wt) and mutant GlyR $\alpha 1$ subunit were used for the *in vitro* synthesis of cRNA (mCAP mRNA Capping Kit; Stratagene, La Jolla, CA, USA) using T7 RNA polymerase as detailed previously (Kondratskaya *et al.* 2005). cRNA concentrations were determined by both measuring the optical density at 260 nm and comparing methylene blue staining intensities after gel electrophoresis.

Electrophysiology

Xenopus laevis oocytes were obtained, and voltage-clamp electrophysiology was performed as described previously (Maksay *et al.* 1999; Grudzinska *et al.* 2005). Animals were handled according to German law (licence no. V 54–19c20/15-F126/13; Regierungspräsidium Darmstadt). Agonist dose–response curves were recorded from cRNA injected oocytes under voltage-clamp conditions and fitted via GraphPad Prism 4 (GraphPad Software Inc., San Diego,

CA, USA) as detailed previously (Grudzinska *et al.* 2005, 2008). Solution exchange was mediated by the BPS drug application system (Adams and List, Westbury, NY, USA) with a flow rate of 0.5 mL/s resulting in a half-exchange time of < 200 ms. Glycine and taurine were co-applied with MBN with or without 30 s of pre-treatment. Inhibitory concentrations of MBN and glycine concentrations corresponding to its half-maximal effect (EC_{50}) were used to determine half-maximal inhibitory concentrations (IC_{50}). Potentiation by MBN was examined with taurine at 10% of the maximal effect (EC_{10}). Data represent mean \pm SEM and were analysed using the KaleidaGraph program (Synergy Software, Reading, PA, USA). Statistical significance was determined by Student's *t*-test and considered to be significant at $p < 0.01$.

Receptor modelling, MBN docking and molecular dynamics simulations

Homology models of the LBDs of $\alpha 1$ GlyRs were generated by using the crystal structures of AChBP (Protein Data Bank code: 1I9B) and nicotinic acetylcholine receptor (2BG9) as templates. The sequences of *Lymnaea stagnalis* AChBP, nicotinic acetylcholine receptor and the LBD of human $\alpha 1$ GlyRs were aligned by Clustal-W and adjusted on the basis of multisequence alignments of Cys-loop receptors (Thompson *et al.* 1994). The program Composer included in the Sybyl 7.0 package (Blundell *et al.* 1988) was used to generate homology models of $\alpha 1$ GlyR-LBDs. AChBP (1I9B) was used as a template for the closed $\alpha 1$ GlyR-LBD model when co-crystallized HEPES molecules were replaced for MBN in the binding interfaces. The GlyR model based on nicotinic acetylcholine receptors (2BG9) was used as a reference structure. The resulting models were refined within Sybyl by alternating short (10–100 fs) molecular dynamics (MD) simulations and energy minimization steps *in vacuo* (Tripos force field, Gasteiger-Hückel charges). MBN was docked using Dock (Sybyl module) and FlexX (Tripos, BioSolveIT, GmbH, Sankt Augustin, Germany) respectively (Rarey *et al.* 1996). The protein-ligand complexes with lowest potential energies were then used as starting structures for MD simulations.

Pentameric $\alpha 1$ GlyR-LBDs with five docked MBN molecules were subjected to MD simulations by GROMACS (Berendsen *et al.* 1995) by using the following parameters: free MD with periodic boundary conditions, gmx force field, isobaric-isothermal ensemble, explicit solvent (spc water model), particle-mesh Ewald electrostatics, Berendsen temperature and pressure coupling, isotropic. The ligand topology of MBN was generated by using the Dundee PRODRG2 web server (Van Aalten *et al.* 1996). To obtain the most important protein-ligand interactions during a MD simulation, the respective parts of the trajectory exhibiting the lowest interaction energies of MBN with $\alpha 1$ GlyR LBDs were averaged and energy-minimized.

Results

To identify determinants of MBN inhibition and potentiation, we injected *X. laevis* oocytes with human wt or mutant $\alpha 1$ GlyR cRNAs. One to 2 days after injection, the oocytes responded to saturating glycine concentrations with chloride currents of 10–50 μ A. GlyR currents could also be elicited by the partial agonist taurine (Schmieden *et al.* 1992). Taurine responses were used to investigate MBN potentia-

tion, as (i) the efficacy of taurine can indicate the effect of mutations on coupling efficiency between agonist binding and activation; and (ii) allosteric modulation of native GlyRs in spinal cord membranes has been more efficacious for partial rather than full agonists (Bíró and Maksay 2004).

Effects of binding site mutations on MBN inhibition

The inhibitory potencies of MBN were examined at previously characterized mutant $\alpha 1$ GlyRs that carry point mutations within the LBD by recording glycine currents at the EC_{50} concentrations previously determined for the respective mutant receptors (Grudzinska *et al.* 2005). MBN alone did not elicit chloride currents. MBN was either pre-incubated for 30 s or co-incubated with glycine. Pre-incubation with subnanomolar MBN (0.2 and 0.5 nM, up to 10 min) did not alter the responses of glycine and did not significantly affect the IC_{50} value of co-incubated MBN. Therefore co-incubation was applied subsequently. Glycine responses of the wt $\alpha 1$ GlyR were inhibited by MBN with an IC_{50} value of 1.5 μ M (Fig. 1 and Table 1). The substitution F63A localized in loop D abolished inhibition by MBN while two other loop D mutations, R65A and Q67A, had no significant effect on inhibitory potency (Fig. 1 and Table 1). Mutations N46C, N102A (loop A), K200A, Y202L and F207A (all in loop C) eliminated the potency of MBN to inhibit glycine currents, whereas R131A (β strand/loop E) and E157C (loop B) increased its IC_{50} by about 20-fold (Table 1). Substitutions in loop E: S129A and R119A had no significant effect. Surprisingly, no inhibition was observed for R119K, a conservative mutation. In conclusion, most of the binding site mutations analysed either reduced or abolished inhibition by MBN.

Effect of binding site mutations on potentiation by MBN

As potentiation by MBN was studied in combination with activation by taurine, the relative efficacy of this partial agonist was compared to that of the full agonist glycine. As it has been shown previously for some of these binding site mutations (Grudzinska *et al.* 2005) they affect the efficacy of taurine. Efficacy varied between 83% for R65A and 7% for R119A $\alpha 1$ GlyRs (Table 1).

In another set of experiments, the chloride currents of the wt and mutant $\alpha 1$ GlyRs elicited by taurine at the respective EC_{10} concentration were recorded following pre-incubation of the oocytes with MBN. The representative current traces shown in Fig. 2(a) illustrate that nanomolar MBN produced small but significant potentiation of the wt $\alpha 1$ GlyR, while at 2 μ M MBN potentiation was obscured by the inhibitory effects of the compound. In contrast, the R131A $\alpha 1$ GlyR showed highly significant potentiation at 2 μ M MBN, which was much larger than the potentiation of the wt GlyR seen at 2 nM MBN. Apparently, reduced inhibition resulting from the R131A substitution (see Fig. 1c) permitted potentiation at micromolar MBN concentrations (see Fig. 2b). Table 1

Table 1 Inhibitory potencies of and potentiation of wt and mutant $\alpha 1$ GlyRs by MBN

cRNA injected	Inhibition by MBN ^a (IC ₅₀) (μ M)	$I_{\max, \text{tau}} / I_{\max, \text{gly}}$ [FRACTION] \times 100	Potentiation by MBN ^b	
			2 nM (%)	2 μ M (%)
wt	1.5 \pm 0.3 (8)	25 \pm 9 ^c	121 \pm 2** (8)	108 \pm 3 (7)
N46C	\gg 100* (4)	50 \pm 4*	158 \pm 11** (4)	127 \pm 7 (5)
F63A	\gg 100* (6)	20 \pm 5 ^c	141 \pm 11** (16)	124 \pm 8 (12)
R65A	1.4 \pm 0.3 (10)	83 \pm 19* ^c	121 \pm 4** (8)	194 \pm 13* (6)
Q67A	0.8 \pm 0.2 (5)	34 \pm 5	102 \pm 4 (5)	83 \pm 6* (5)
N102A	\gg 100* (3)	26 \pm 3	176 \pm 9** (4)	246 \pm 34* (4)
R119A	2.5 \pm 1.1 (6)	7 \pm 1* ^c	91 \pm 4 (6)	<100
R119K	\gg 100* (5)	37 \pm 15	142 \pm 14 (6)	423 \pm 52* (4)
S129A	3.4 \pm 1.2 (5)	51 \pm 6	110 \pm 2 (5)	54 \pm 15* (4)
R131A	30 \pm 4* (5)	65 \pm 10* ^c	123 \pm 3** (12)	199 \pm 21* (8)
E157C	23 \pm 12* (4)	21 \pm 6	129 \pm 8** (4)	187 \pm 29* (3)
K200A	\gg 100* (5)	17 \pm 9	182 \pm 23** (6)	298 \pm 91* (3)
Y202L ^d	\gg 100* (6)	23 \pm 10	114 \pm 2** (6)	148 \pm 29 (4)
F207A	\gg 100* (7)	37 \pm 12	94 \pm 3 (7)	212 \pm 35* (3)

Data are mean \pm SEM from *n* (indicated in brackets) oocytes. Efficacies were determined with 4–6 oocytes.

GlyRs, glycine receptors; MBN, 3 α -(3'-methoxy-benzoyloxy)nortropane; IC₅₀, half-maximal inhibitory concentrations.

^aDetermined at the respective EC₅₀ values of glycine.

^bEnhancement by MBN of $\alpha 1$ GlyR currents elicited by the respective EC₁₀ concentrations of taurine.

^cTaken from Grudzinska *et al.* (2005).

^dLow taurine activity. Y202A was not functional.

*Significantly different ($p < 0.01$) from wt $\alpha 1$ GlyRs (unpaired Student's *t*-test).

**Current enhancement by MBN was significant ($p < 0.001$) over control (unpaired Student's *t*-test).

shows that the point mutations N46C, F63A, R119K, R131A, E157C and K200A which all eliminate or reduce inhibition generated GlyRs that were significantly potentiated by MBN. With the inhibition-deficient mutants: N102A, R119K and K200A, MBN potentiation was even enhanced (Table 1). In contrast, mutations Q67A, R119A and S129A eliminated MBN potentiation (Table 1). Most of the mutations which did not affect potentiation by 2 nM MBN (Table 1) showed enhanced potentiation at micromolar MBN as demonstrated for the R131A GlyR in Fig. 2b.

MD simulations suggest different binding modes for inhibition and potentiation

The effects of the binding site mutations described above indicate that MBN interacts with the $\alpha 1$ GlyR-LBD in the agonist-binding site formed between subunit interfaces. We therefore used a structural model of the pentameric extracellular domain of the $\alpha 1$ GlyR to dock MBN into the LBDs formed at the interfaces of wt and mutant $\alpha 1$ GlyR subunits. The docked structures were subsequently subjected to MD simulations. We paid primary attention to the rearrangements of loop C in concert with MBN. The MD simulations revealed that MBN might adopt two different positions in the agonist-binding cavity of the $\alpha 1$ GlyR. One position of MBN accompanied with permanent outward pushing of loop C to half-open conformation was associated with inhibition, while another position with inward motion (closure) of loop

C was associated with potentiation. Notably, these MD simulations then led to MBN positions with the lowest energy.

3 α -(3'-methoxy-benzoyloxy)nortropane was docked in the closed $\alpha 1$ GlyR-LBD model. The most stable docking position of MBN predicted from 20 ns MD simulation resulted in a ligand-LBD complex (Fig. 3, top left) with a binding energy of -258 kJ/mol. Here, MBN penetrated deeply in the interface cavity below the lower (cellular) side of loop C. It was in close contact with amino acid side chains whose mutations affected MBN inhibition, therefore we consider it 'inhibitory' binding. Accordingly, MBN could interact with residues N46, N102, F159 and, like strychnine (Grudzinska *et al.* 2005), with F63 and R131 (Fig. 3, top left). In this docking position, MBN is distant from residue R65, in agreement with the inability of mutation R65A to affect inhibition. The nortropane head is nested in a hydrophilic vestibule. Its secondary amino group is in hydrogen-bonding distance to the asparagines N102 in loop A and N46, while the carbonyloxy moiety of MBN seems to form strong hydrogen bonds with R131 in loop E. Notably, in this docking orientation the aromatic ring of MBN sits in a cleft between the aromatic rings of F63 and F159 intercalated as a wedge and suitable for π - π interactions. MD simulations suggest that the conformation of loop C is stabilized by interactions within the principal subunit: E157 with K200 and Y202 as well as π - π interactions between Y202 and

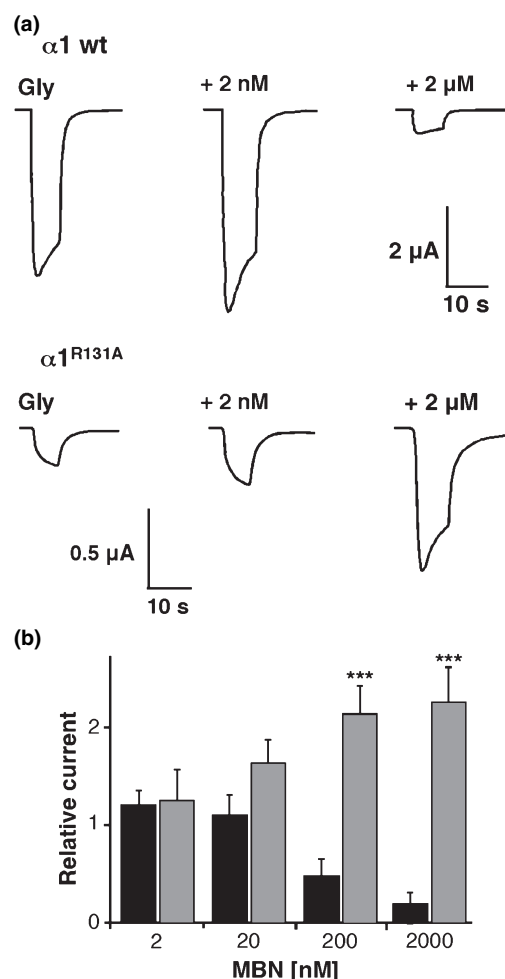


Fig. 2 Inhibition and potentiation of the wt and R131A GlyRs by MBN. (a) Representative current traces. Oocytes were pre-incubated with the indicated concentrations of MBN for 30 s followed by the application of taurine at the respective EC_{10} concentration. (b) Concentration dependence of MBN modulation of the wt and R131A GlyRs represented by black and grey columns respectively. Data are mean \pm SEM from 5 to 10 oocytes. Note potentiation of the R131A receptor by MBN concentrations that inhibit wt $\alpha 1$ GlyRs. ***Significant enhancement ($p < 0.01$).

F207. This docking position of MBN seems to prevent interface interactions and hinder the full closure of loop C that would elicit channel gating. This half-shut conformation lies in-between the agonist-bound (closed) and non-liganded (open) conformations. The superimposed structures shown in Fig. 3 (left bottom) also indicate the conformation-specific distances between the respective $C\alpha$ atom positions of N203 at the tip of loop C.

To further explore the role of N102 in MBN binding and inhibition of $\alpha 1$ GlyRs, we also modelled the mutated N102A GlyR-LBD in order to determine whether mutation N102A not only impairs inhibition but also the docking stability of MBN. MD simulations were performed with

MBN-docked pentameric $\alpha 1$ wt and N102A GlyR-LBDs under identical conditions. The compactness of a cylindrical pentamer can be characterized by its radius of gyration (Rg) of the backbone atoms. As the core structure of the pentamer was very stable, changes in Rg should mainly reflect conformational flexibility of loop C and the size of the binding cavity underneath it. With MBN docked below loop C and the NH moiety of MBN pointing to N102, the Rg value of the wt $\alpha 1$ GlyR increased from 2.90 to 2.92 nm, while the Rg of the N102A mutant declined substantially below 2.86 nm within 20 ns MD simulation (not shown). The Rgs were subsequently dissected into those of core pentamers (without loops C) and of loops C themselves. These MD simulations are illustrated in Fig. S1, where the time-dependent changes of the Rg values of loops C alone are plotted. The substantial difference of about 0.2 nm in Rg between loops C of wt $\alpha 1$ and N102A GlyRs reflects different loop C positions, with MBN being docked stably under the half-shut loop C of the wt receptor, whilst in N102A GlyRs the distorted interface cavity might collapse. We also measured the distance of the nortropane N atom of docked MBN from $C\alpha$ atoms of N102 and of N102A following 20 ns MD simulation. The average distance of MBN was about 0.2 nm greater from N102A than from N102 (not shown). This indicates that MBN moved away from the mutated N102A parallel with the collapse of the binding cavity during MD simulation while it was tightly bound to N102. These findings support the suitability of MD simulations and underline the crucial role of N102 in MBN binding and inhibition of $\alpha 1$ GlyRs.

Our MD simulations also disclosed a second, even more stable docking position, whose ligand interactions can be reconciled with the mutations affecting MBN potentiation (Fig. 3, top right and centre). This position was obtained after docking MBN into a half-shut LBD structure, followed by MD simulation for 20 ns. In the course of MD simulation, MBN rotated clockwise by about 30° (seen from outside), relocated towards the centre of the LBD by about 0.4 nm and apposed to the inner surface of loop C. In this docking orientation with a calculated binding energy of -288 kJ/mol, the aromatic ring of MBN was buried in a hydrophobic cleft formed by residues F63, F159, Y202 and F207, while the nortropane NH group was close to residues Q67, R119 and S129 (Fig. 3, top right). If R119 is replaced for K, the Lys side chain which is more flexible than that of Arg might accommodate MBN at the potentiating site preferentially over the inhibitory site. This might explain the preferential potentiation of R119K $\alpha 1$ GlyRs.

In the 'potentiating' MBN-bound structure loop C adopted a closed conformation that appears to be stabilized by interactions with both MBN and side chains of the complementary (-)face of the binding site (data not shown). The resulting structure (Fig. 3, bottom right) strongly resembles

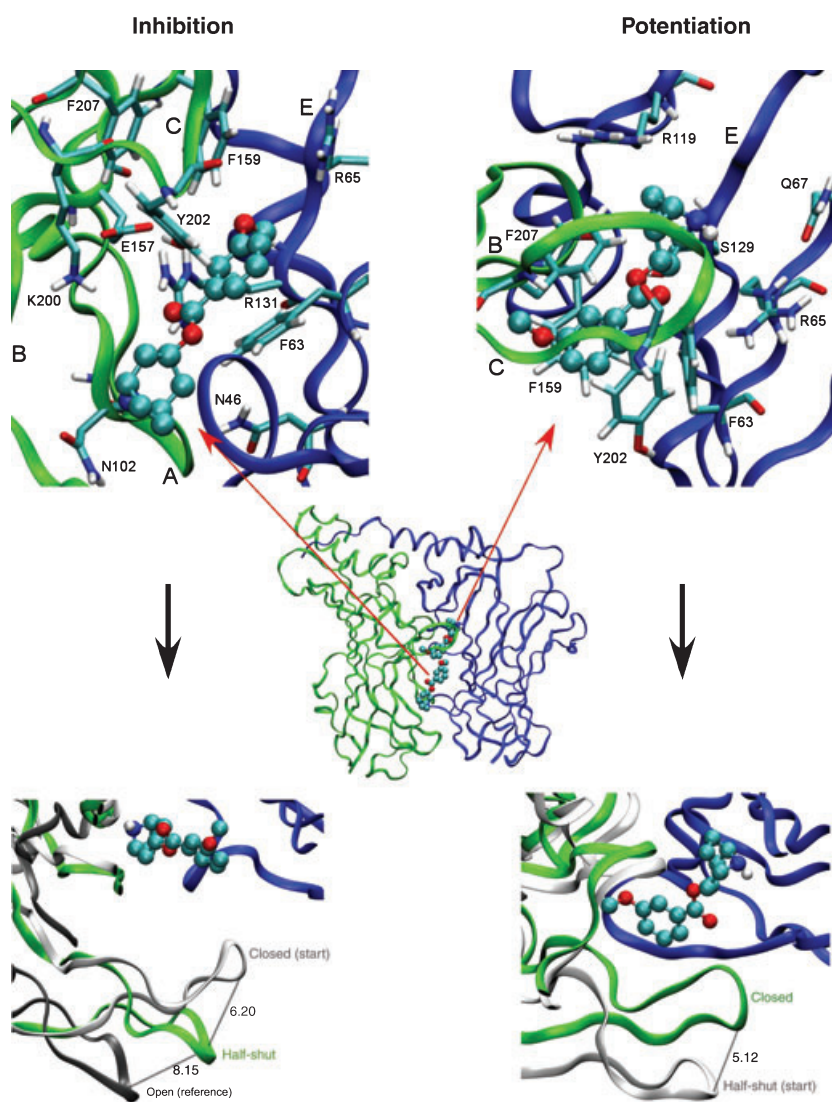


Fig. 3 Docking modes of MBN (ball and stick representation) in the LBD of $\alpha 1$ GlyRs. The central panel shows LBDs of two adjacent $\alpha 1$ GlyR subunits in green and blue with MBN docked in two positions correlated with inhibition and potentiation respectively. Top, left and right enlargements show the side chain interactions involved in MBN binding for the presumptive inhibitory and potentiating binding modes respectively. The potentiating docking mode of MBN is 'above' the inhibitory one by about 1 nm. It also differs by twofold rotations of about 180° around the y and z axes respectively. Bottom, left and right panels illustrate loop C positions (in green) for the two modes of MBN docking following MD simulations (top view). Loops C overlaid in white refer to the MD starting points. MD simulations of inhibition and potentiation started from closed and half-shut LBDs respectively. The bottom left panel demonstrates that MD simulation with MBN docked in the inhibitory orientation opens loop C half-way as compared with the non-liganded open (reference) loop C position overlaid in black.

the agonist-liganded LBD, and hence might facilitate channel opening.

Discussion

In this study, mutations within the agonist-binding site of the $\alpha 1$ GlyR are shown to affect potentiation and/or inhibition of the recombinant homomeric receptor by a representative tropeine, MBN. This result strongly supports the view that the biphasic modulatory effects of tropeines are mediated at the agonist-binding cavity localized at subunit interfaces, with low and high agonist and modulator occupancies resulting in potentiation and inhibition respectively.

Determinants of MBN inhibition and potentiation

Several GlyR $\alpha 1$ substitutions previously shown to increase the EC_{50} of glycine and other agonists were found here to affect MBN inhibition of glycine responses. Notably, these substitutions were localized in four of the six subdomains

which form the agonist-binding site between adjacent subunits of the homomeric $\alpha 1$ receptor. Specifically, the mutations N102A in loop A; E157C in loop B; K200A, Y202L and F207A in loop C; R119K and R131A in β strand E respectively, all strongly reduced or eliminated MBN inhibition. The N102A substitution has been found to abolish inhibition of glycine responses by the closely related tropeine tropisetron (Yang *et al.* 2007). However, in that study other mutations at the ligand-binding site had no effect on tropisetron inhibition. Notably, substitutions of residues E157, Y202 and F207 have been shown to also impair the inhibition of $\alpha 1$ GlyR currents by Zn^{2+} and Cu^{2+} (Grudzinska *et al.* 2008; Schumann *et al.* 2008). Thus, (partly) common binding site residues appear to be implicated in the inhibition of glycine responses by both tropeines and divalent metal ions.

Only few of the mutations that did not affect inhibition impaired potentiation by MBN. Specifically, substitutions Q67A, R119A and S129A eliminated potentiation by MBN. In contrast, several mutations which abolished or attenuated

inhibition: N46C, F63A, N102A, R119K, R131A, E157C and K200A all maintained or enhanced GlyR potentiation by MBN. Some of these mutations which attenuated MBN inhibition (N102A, R131A, E157C and K200A) showed enhanced potentiation at micromolar MBN, consistent with impaired inhibition unmasking GlyR potentiation at higher modulator occupancy. Substitutions of residue F207 have also been found to affect inhibition and, importantly, potentiation by divalent metal ions (Grudzinska *et al.* 2008; Schumann *et al.* 2008). The side chain of F207 thus seems to constitute a crucial determinant of modulator action. Interestingly, R119 appears to function as a switch between inhibition and potentiation by MBN depending on its replacement. The R119A $\alpha 1$ GlyR was invariably inhibited by MBN while it was activated by taurine with very low efficacy which could not be potentiated by MBN. In contrast, the R119K $\alpha 1$ GlyR was not inhibited by MBN while its activation by taurine was potentiated by MBN to the greatest extent.

No linear correlation can be observed between the efficacy of taurine and potentiation by 2 nM MBN ($r^2 = 0.008$) and 2 μ M MBN ($r^2 = 0.0003$). This suggests that the mutations did not affect MBN potentiation indirectly by modifying agonist binding.

Different docking positions of MBN predicted by MD simulation

The effects of our point mutations on MBN potentiation and inhibition indicate that both binding sites of tropeines are located at the subunit interface cavities of the $\alpha 1$ GlyR. The potentiating binding of MBN appears to overlap with glycine binding while inhibition requires MBN binding next to it as shown in Fig. 3. Our docking studies and MD simulations strongly suggest that MBN can adopt different positions and that these different docking modes are associated with distinct effects, i.e. potentiation and inhibition of GlyR currents. As the binding cavities of ionotropic Cys-loop and glutamate receptors are closed upon binding of agonists whereas antagonists prevent, or allow only partial closure (Furukawa and Gouaux 2003; Hansen *et al.* 2005), we propose that comparable differences in binding site conformations also underlie MBN potentiation and inhibition respectively. Moreover, the different binding energies and C loop orientations predicted for the two MBN binding modes can be attributed to the different efficacies of MBN: the higher binding energy of MBN docking with a closed loop C position can be associated with high-affinity potentiation, whilst the docking mode of lower binding energy with low-affinity inhibition.

It is informative to compare MBN binding with the binding of agonists and antagonists to GlyRs and other Cys-loop receptors. Glycine binding and activation of $\alpha 1$ GlyRs requires cation- π interaction of the amino group of glycine with residue F159 (Pless *et al.* 2008) and ionic interaction of its carboxylate group with R65 (Grudzinska *et al.* 2005).

Inhibition of $\alpha 1$ GlyRs by tropisetron is abolished by mutations of N102, and it has been proposed that the tropane head interacts with residue N102 (Yang *et al.* 2007). Tropeine antagonism of 5-HT_{3A} receptors is attenuated upon mutation of W89 (Yan *et al.* 1999), a residue homologous to F63 in $\alpha 1$ GlyRs. Granisetron binding to 5-HT_{3A} receptors could be localized under both arms of loop C (Joshi *et al.* 2006). These findings support the existence of binding cavities of tropeines on GlyRs and 5-HT₃ receptors in common with those of their agonists.

The conformational changes underlying GlyR potentiation are not fully understood. It is generally assumed that multiple subunit interface sites must be occupied in order to cause efficient channel opening of Cys-loop receptors such as of GABA_A receptors via binding of GABA and benzodiazepines (Hanson and Czajkowski 2008). Potentiating binding of tropeines apparently occurs in the glycine-binding cavities, in the GlyRs interface. Closure of loops C around glycine bound at one interface, and around tropeines bound at another interface, may lead to allosteric facilitation of binding and channel opening, as known for GABA and benzodiazepines at GABA_A receptors (Hanson and Czajkowski 2008). At high tropeine occupancy inhibition will predominate over potentiation. Elucidation of the distinct binding modes of modulators will hopefully lead to therapeutic agents with preferential potentiation over inhibition of Cys-loop receptors.

Acknowledgements

We thank Professor Péter Nemes (Szent István University, Budapest) for the synthesis of MBN and Tanja Schumann for experimental contributions. This study was supported by grants K-62203 (OTKA) and D-32 (Hungarian-German Intergovernmental S & T Cooperation Programme) to GM, Gemeinnützige Hertie-Stiftung to BL, Max-Planck-Gesellschaft, Deutsche Forschungsgemeinschaft (EXC 115) and Fonds der Chemischen Industrie to HB.

Supporting information

Additional Supporting Information may be found in the online version of this article:

Figure S1 Plot of the radii of gyration (Rg) of backbone atoms of loops C of MBN-docked $\alpha 1$ wt and N102A GlyRs based on MD simulations under identical conditions. Rgs of $\alpha 1$ GlyRs were dissected into those of core pentamers without loops C and of the backbones of loops C alone, and Rgs of only loops C are plotted. Note the increase of 0.08 nm in Rg values of the wt loop C upon MBN docking, whereas the Rg of N102A loop C declined by 0.04 nm during 20 ns MD simulation.

Please note: Wiley-Blackwell are not responsible for the content or functionality of any supporting materials supplied by the authors. Any queries (other than missing material) should be directed to the corresponding author for the article.

References

- Aprison M. H. (1990) The discovery of the neurotransmitter role of glycine, in *Glycine Neurotransmission* (Ottersen O. P. and Storm-Mathiesen J., eds), pp. 1–23. John Wiley and Sons Ltd, New York.
- Becker C. M., Hoch W. and Betz H. (1988) Glycine receptor heterogeneity in spinal cord during postnatal development. *EMBO J.* **7**, 3717–3726.
- Beckstead M. J., Phelan R., Trudell J. R., Bianchini M. J. and Mihic S. J. (2002) Anesthetic and ethanol effects on spontaneously opening glycine receptor channels. *J. Neurochem.* **82**, 1343–1351.
- Berendsen H. J. C., van der Spoel D. and van Drunen R. (1995) GROMACS: a message-passing parallel molecular dynamics implementation. *Comp. Phys. Commun.* **91**, 43–56.
- Bíró T. and Maksay G. (2004) Allosteric modulation of glycine receptors is more efficacious for partial rather than full agonists. *Neurochem. Int.* **44**, 521–527.
- Blundell T. L., Carney D., Gardner S., Hayes F., Howlin B., Hubbard T., Overington J., Singh D. A., Sibanda B. L. and Sutcliffe M. J. (1988) Knowledge-based protein modeling and design. *Eur. J. Biochem.* **172**, 513–520.
- Brejč K., Van Dijk W., Klaassen R. V., Schuurmans M., Van der Oost J., Smit A. B. and Sixma T. K. (2001) Crystal structure of an ACh-binding protein reveals the ligand-binding domain of nicotinic receptors. *Nature* **411**, 269–276.
- Celie P. H., van Rossum-Fikkert S. E., van Dijk W. J., Brejč K., Smit A. B. and Sixma T. K. (2004) Nicotine and carbamylcholine binding to nicotinic acetylcholine receptors as studied in AChBP crystal structures. *Neuron* **41**, 907–914.
- Changeux J. P. and Taly A. (2008) Nicotinic receptors, allosteric proteins and medicine. *Trends Mol. Med.* **14**, 93–102.
- Chesnoy-Marchais D. (1996) Potentiation of chloride responses to glycine by three 5-HT₃ antagonists in rat spinal neurones. *Br. J. Pharmacol.* **118**, 2115–2125.
- Furukawa H. and Gouaux E. (2003) Mechanisms of activation, inhibition and specificity: crystal structures of the NMDA receptor NR1 ligand-binding core. *EMBO J.* **22**, 2873–2885.
- Grudzinska J., Schemm R., Haeger S., Nicke A., Schmalzing G., Betz H. and Laube B. (2005) The β subunit determines the ligand binding properties of synaptic glycine receptors. *Neuron* **45**, 1–13.
- Grudzinska J., Schumann T., Schemm R., Betz H. and Laube B. (2008) Mutations within the agonist-binding site convert the homomeric $\alpha 1$ glycine receptor into a Zn²⁺-activated chloride channel. *Channels* **2**, 13–18.
- Hansen S. B., Sulzenbacher G., Huxford T., Marchot P., Taylor P. and Bourne Y. R. (2005) Structures of alypsia AChBP complexes with nicotinic agonists and antagonists reveal distinctive binding interfaces and conformations. *EMBO J.* **24**, 3635–3646.
- Hanson S. M. and Czajkowski C. (2008) Structural mechanisms underlying benzodiazepine modulation of the GABA_A receptor. *J. Neurosci.* **28**, 3490–3499.
- Harvey R. J., Depner U. B., Wässle H. *et al.* (2004) GlyR $\alpha 3$: An essential target for spinal PGE₂-mediated inflammatory pain sensitization. *Science* **304**, 884–887.
- Joshi P. R., Suryanarayanan A., Hazai E., Schulte M. K., Maksay G. and Bikádi Z. (2006) Interactions of granisetron with an agonist-free 5-HT_{3A} receptor model. *Biochemistry* **45**, 1099–1105.
- Kondratskaya E., Betz H., Krishtal O. and Laube B. (2005) The β subunit increases the ginkgolide B sensitivity of inhibitory glycine receptors. *Neuropharmacology* **49**, 945–951.
- Laube B., Maksay G., Schemm R. and Betz H. (2002) Modulation of glycine receptor function: a novel approach for the therapeutic intervention at inhibitory synapses? *Trends Pharmacol. Sci.* **23**, 519–527.
- Lynch J. W. (2004) Molecular structure and function of the glycine receptor chloride channel. *Physiol. Rev.* **84**, 1051–1095.
- Maksay G. (1998) Bidirectional allosteric modulation of strychnine-sensitive glycine receptors by tropeines and 5-HT₃ serotonin receptor ligands. *Neuropharmacology* **37**, 1633–1641.
- Maksay G., Laube B. and Betz H. (1999) Selective blocking effects of tropisetron and atropine on recombinant glycine receptors. *J. Neurochem.* **73**, 802–806.
- Maksay G., Nemes P. and Bíró T. (2004) Synthesis and allosteric modulation of ionotropic glycine receptors. *J. Med. Chem.* **47**, 6384–6391.
- Maksay G., Bíró T., Laube B. and Nemes P. (2008) Hyperekplexia mutation R271L of $\alpha 1$ glycine receptors potentiates allosteric interactions of nortropeines, propofol and glycine with [³H]strychnine binding. *Neurochem. Int.* **52**, 235–240.
- Nevin S. T., Cromer B. A., Haddrill J. L., Morton C. J., Parker M. W. and Lynch J. W. (2003) Insights into the structural basis for zinc inhibition of the glycine receptor. *J. Biol. Chem.* **278**, 28985–28992.
- Pless S. A., Millen K. S., Hanek A. P., Lynch J. W., Lester H. A., Lummis S. C. R. and Dougherty D. A. (2008) A cation- π interaction in the binding site of the glycine receptor is mediated by a phenylalanine residue. *J. Neurosci.* **28**, 10937–10942.
- Rarey M., Kramer B., Lengauer T. and Klebe G. (1996) A fast flexible docking method using an incremental construction algorithm. *J. Mol. Biol.* **261**, 470–489.
- Schmiedon V., Kuhse J. and Betz H. (1992) Agonist pharmacology of neonatal and adult glycine receptor alpha subunits. Identification of amino acid residues involved in taurine activation. *EMBO J.* **11**, 2025–2032.
- Schumann T., Grudzinska J., Kuzmin D., Betz H. and Laube B. (2008) Binding-site mutations in the $\alpha 1$ subunit of the inhibitory glycine receptor convert the inhibitory metal ion Cu²⁺ into a positive modulator. *Neuropharmacology* **56**, 310–317.
- Thompson J. D., Higgins D. G. and Gibson T. J. (1994) Clustal-W – improving the sensitivity of progressive multiple sequence alignment through sequence weighting, position-specific gap penalties and weight matrix choice. *Nucleic Acids Res.* **22**, 4673–4680.
- Van Aalten D. M. F., Bywater R., Findlay J. B. C., Hendlich M., Hoofst R. W. W. and Vriend G. (1996) PRODRG, a program for generating molecular topologies and unique molecular descriptors from coordinates of small molecules. *J. Comput. Aided Mol. Des.* **10**, 255–262.
- Yan D., Schulte M. K., Bloom K. E. and White M. M. (1999) Structural features of the ligand-binding domain of the serotonin 5HT₃ receptor. *J. Biol. Chem.* **274**, 5537–5541.
- Yang Z., Ney A., Cromer B. A., Ng H. L., Parker M. W. and Lynch J. W. (2007) Tropisetron modulation of the glycine receptor: femtomolar potentiation and a molecular determinant of inhibition. *J. Neurochem.* **100**, 758–769.
- Yang Z., Aubrey K. R., Alroy I., Harvey R. J., Vandenberg R. J. and Lynch J. W. (2008) Subunit-specific modulation of glycine receptors by cannabinoids and N-arachidonyl-glycine. *Biochem. Pharmacol.* **76**, 1014–1023.